American Scientific Research Journal for Engineering, Technology, and Sciences (ASRJETS)

ISSN (Print) 2313-4410, ISSN (Online) 2313-4402



http://asrjetsjournal.org/

# Ignition of Smoldering in Cotton: 3D-Heat-Transfer-Modeling

Bjarne C. Hagen*

*Western Norway University of Applied Sciences, Bjørnsonsgt. 45, N-5528 Haugesund, Norway*

**Abstract**

The temperature and time for onset of smoldering in cotton are estimated using a pure finite element heat-transfer model (Comsol) together with 1D- and 3D-ignition models. A comparison of the simulated results with the experimental results shows that the temperature for onset of smoldering can be estimated to within 2-3% of the experimental results, or within 7-10 °C, using a 3D-ignition model. The time to onset is estimated to within 5% (or 2 minutes) of the experimental result for high heat flux scenarios. For low heat flux scenarios the time estimates are poorer and within approximate 50% of the experimental results. For the 1D-model the results are less accurate and less systematic compared with the experimental results. The results presented here show that simulations of onset of smoldering can be performed using 3D-heat-transfer-models. The model used here is simple to implement and to use in for more practical engineering applications.

***Keywords:*** smoldering; ignition; simulation; 3D; modeling.

## 1. Introduction

The onset of smoldering fire can be caused by different ignition sources such as: glowing embers, flames, hot surfaces and other smoldering materials [1,2]. A substantial work has been performed both experimentally and theoretically to determine the minimum temperature and heat flux causing onset of smoldering. Results show that the minimum ignition temperature for solid materials is dependent on the test apparatus, density, geometry and heat flux [3]. Since there is no minimum ignition temperature for solid materials, computer modeling is an alternative to experiments to determine the onset of smoldering for given heat flux scenarios and geometric configurations.Work done by Suhendra

------------------------------------------------------------------------

* Corresponding author.

Schmidt and Krause [4] shows that smoldering can be modeled using computer models combining reaction kinetics, fluid flow and heat transfer. Similarly Dodd, Lautenberger and Fernandez-Pello have showed that smoldering and transition to flaming can be simulated using the model Gpyro [5]. While Chen, Rein and Liu [6] have investigated the effects of moisture, density and inorganic contents using numerical simulations.This article will investigate the onset of smoldering using a pure finite element heat-transfer-model (Comsol) estimating the temperature within a cotton sample.

From the estimated temperature, the time and temperature for onset of smoldering will be investigated using one dimensional (1D) and three dimensional (3D) ignition models.

The work is an extension of the experimental work done by Hagen and his colleagues [7].

In section 2 previous research on ignition and onset of smoldering will be discussed together with experimental work from Hagen and his colleagues [7]. In section 3 the computer model and simulation input will be presented, and in section 4 the simulation results are presented and compared to the experimental results presented in section 2. In section 5 the results will be discussed.

## 2. Previous research

### *2.1 Ignition theory*

To calculate the temperature for onset of smoldering, one-dimensional ignition models incorporating heat flow and heat generation, have been developed.

The ignition model developed by [8] is a simple one-dimensional model that incorporates heat flow, heat generation and a linear temperature gradient through the sample. This model was then extended by [3] and Hagen and his colleagues [9] to investigate onset of smoldering in cellulose and cotton, respectively.

The main assumption of the model developed by Bowes and Townsend is that immediately before ignition, heat production from the reaction zone balances heat transported to the cooler surroundings. The heat flow balance is given by [3]:

$$\int_V \dot{q}'''_{Generation}\, dV = \int_{S2} \dot{q}''_{Loss}\, dS_2 \qquad (1)$$

The heat flow balance describes a control volume limited by the surfaces S1 and S2 (see figure 1). In the model developed by Bowes and Townshend [8] S1 is the boundary between the hotplate and the fuel which in this article is cotton, while surface S2 is the boundary between the heated cotton and cotton at ambient temperature [10].

This is a one-dimensional heat-transfer-model: heat is only transported up through the cotton and sideways heat loss is not accounted for.

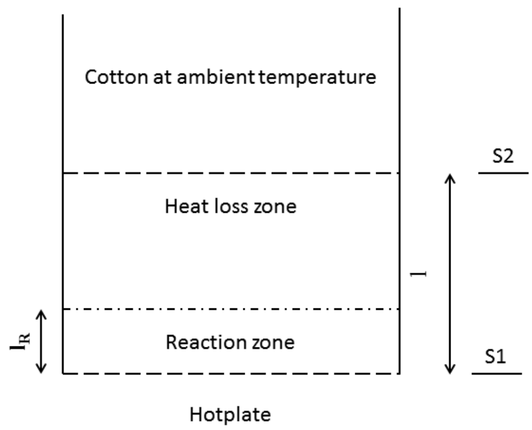


**Figure 1:** Illustration of the one-dimensional heat transfer system.

The first integral in equation 1 gives the heat generated in the cotton and the second integral gives the heat loss. As a first approximation, the heat generation is dependent on the depth (vertical extension) of the sample reaction zone ($l_R$) and the constant temperature in the reaction zone. Ohlemiller showed that with a constant temperature in the reaction zone, the heat generation is approximately given by [3]:

$$\int_V \dot{q}'''_{Generation}\, dV = \Delta H_C\, \rho\, l_R A^* \exp(-E_a / RT_P) \qquad (2)$$

where $\Delta H_C$ is heat of combustion, $\rho$ is density, $A^*$ is a pre-exponential factor, $E_a$ is the activation energy, $R$ is the gas constant, $T_p$ is the hotplate temperature, and $l_R$ is the height of the reaction zone with value [3]:

$$l_R = \frac{R T_P{}^2}{b E_a} \qquad (3)$$

where $b$ is the temperature gradient in the sample.

Ohlemiller's model is based on a stationary situation where the temperatures through a thin sample are independent of time. Hagen and his colleagues [9] adapted Ohlemiller's model but redefined $l$, the height of the hot part of the sample (between S1 and S2 in figure 1), to a constant value of 0.04 m, consistent with the length from the hotplate to the level (height) where the material had room temperature. Hagen and his colleagues [7] then introduced an effective layer depth ($l$) to be used to determine the temperature gradient ($b$) through the material. The effective depth was defined as the distance from the hotplate to the level where the temperature is 40 °C, referred to as $T_{lim}$, the limiting temperature [7].

$$b = \frac{T_P - T_{\lim}}{l} \qquad (4)$$

Near the onset of smoldering is assumed that the heat production is equal to the heat loss due to conduction in the sample, and the ignition temperature ($T_p$) can be found using equation 5.

$$\Delta H_C \, \rho \, l_R \, A^* \exp(-E_a / RT_P) = \frac{k}{l}\left(T_P - T_{\lim}\right) \qquad (5)$$

As reported by Hagen and his colleagues [9] the temperature gradient in a sample differs with time and position in the sample. The ignition models discussed above do not properly account for ignition scenarios where the sample is heated for a long period. For this kind of scenario the sample will behave as a thermally thin object and loose heat through its sides [7]. Similarly, the temperature gradient as a function of position is not well represented by a linear temperature gradient between the hotplate and the limiting temperature [7]. To account for different heat losses and temperature gradients, the use of 3D-heat-transfer-models to simulate the temperature development in a cotton sample should be used. The heat release in cotton varies with temperature, and does not follow an Arrhenius approximation as the temperature increases (see figure 5). A 3D-heat-transfer-model can account for the real heat production as a function of temperature.

### *2.2 Experimental results*

The experiments simulated in this article are described by Hagen and his colleagues [9] . Therefore the sample material, experimental set-up and results will only be discussed briefly.

***2.2.1 Material and experimental set-up***The sample material used in these experiments was cotton batting [9]. Cotton was chosen since it represents a group of cellulose-based materials prone to smoldering. During experiments, the ambient temperature was 15-25 °C and the relative humidity 40-50 %.The experimental set-up is shown in figure 2. The sample was 0.15 m x 0.15 m x 0.15 m. The chosen length and width are discussed in ref. [9]. A hotplate was chosen as the ignition source, since it allows reproducible heating scenarios. In order to reduce effects of air currents, the sample was placed within a container (1.2 m x 0.7 m x 0.6 m) made of light plastic sheets.

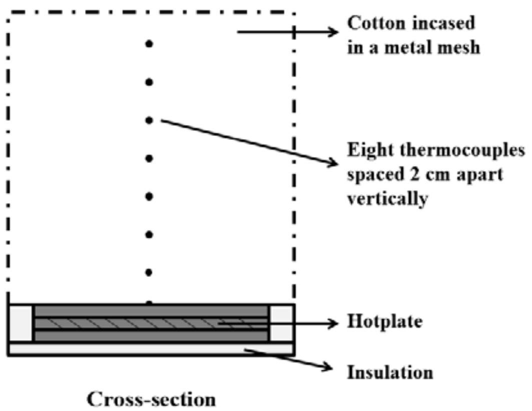


**Figure 2:** Experimental set-up: The cotton sample is incased in a metal mesh. There are placed type K thermocouples every 2 cm along the center line of the sample. The hotplate consists of three ceramic tiles, with an electrical hot-wire wound around the middle one.

Before each experimental run cotton was packed to a predefined density and thermocouples placed within the sample. If an experiment did not result in smoldering, the cotton was reused. However, the cotton close to the hotplate was replaced after a previous no-ignition experiment since this layer was partly decomposed. The amount of cotton replaced was based on changes in color and texture. In most cases only the lower 2 cm of cotton was replaced.

To monitor the temperature, a type K thermocouple was placed directly on top of the hotplate. In addition, seven thermocouples were used to measure the temperature within the sample. The thermocouples were 2 cm apart along the vertical centerline of the sample. The thermocouples used had a diameter of 0.5 mm including the outer casing.

### *2.2.2 Scenario and results*

Hagen and his colleagues [7] investigated experimentally six heating scenarios and five densities of cotton. In this article cotton with density 100 kg/m$^3$ will be investigated together with four heat flux scenarios. The two scenarios not included are one where the cotton is reheated until onset occurs and the other is a combination of scenario A and D. **Scenario A. High heat flux (12.8 kW/m$^2$) followed by cooling**: The hotplate was heated to a pre-determined temperature (called the cut-off temperature), and then switched off. A heat flux of 12.8 kW/m$^2$ (the maximum allowed by the current set-up) was used, resulting in a temperature rise of 20-30 °C pr. minute at the top of the hotplate (see figure 3). In figure 3a the power was switched off as the hotplate temperature (upper curve) reached 275 °C, while the maximum recorded hotplate temperature was 303 °C. The temperature profile in figure 3a is typical for a non-smoldering experiment: here the hotplate and the sample cool after reaching a maximum temperature. In figure 3b the power was switched off as the hotplate temperature (upper curve) reached 280 °C, and the increased hotplate temperature (as compared with the case in figure 3a) resulted in ignition. Here the hotplate does not cool, due to the heat production of the smoldering fire, and high temperatures are reached throughout the sample. The hotplate was heated using a hotwire. The different heat flux scenarios are described according to how much energy is given off by the hotplate. The amount of energy transported in the hotwire is divided by the total area of the hotplate. For scenario A 285 W is used to heat the hotwire, and divided by the hotplate area of 0.0223 m$^2$ gives 12.8 kW/m$^2$.

**Scenario B. Medium high heat flux (4.5 kW/m$^2$) followed by cooling**: The hotplate was heated to a pre-determined temperature, and then switched off. A heat flux of 4.5 kW/m$^2$ (35% of the flux for scenario A) was used, resulting in a temperature rise of 7 °C pr. minute at the top of the hotplate. In figure 3c the hotplate was switched off when the temperature reached 305 °C, giving a maximum temperature of 311 °C which did not cause ignition. In figure 3d the hotplate reached a maximum temperature of 316 °C initiating smoldering.

**Scenario C. Medium low heat flux (2.2 kW/m$^2$) followed by cooling:** The hotplate was heated to a pre-determined temperature, and then switched off. A heat flux of 2.2 kW/m$^2$ (18% of the flux for scenario A) was used, resulting in a temperature rise of 3 °C pr. minute at the top of the hotplate. The temperature curves for a non-smoldering case are shown in figure 3e. The hotplate reached a maximum temperature of 312 °C, with no smoldering. In figure 3f the hotplate was switched off at 315 °C. In this case the temperature did not stabilize and smoldering occurred. **Scenario D. Low constant heat flux**: The sample was heated using a low constant heat flux. Figure 3g shows the temperature development for an experiment where the power was held constant at 1.43 kW/m$^2$, resulting in a maximum hotplate temperature of 279 °C with no smoldering ignition. Due to the constant heat flux, the temperature stays constant after a maximum temperature has been reached, in contrast to the non-smoldering cases in scenarios A-C, where the temperature is reduced after the hotplate has been switched off. An increase in the power input to 1.52 kW/m$^2$ resulted in ignition, as shown in figure 3h. Time and temperature for onset of smoldering for the experiments, are shown in table 1 [7]. The results show that the onset of smoldering is dependent on the heating scenario of the cotton.

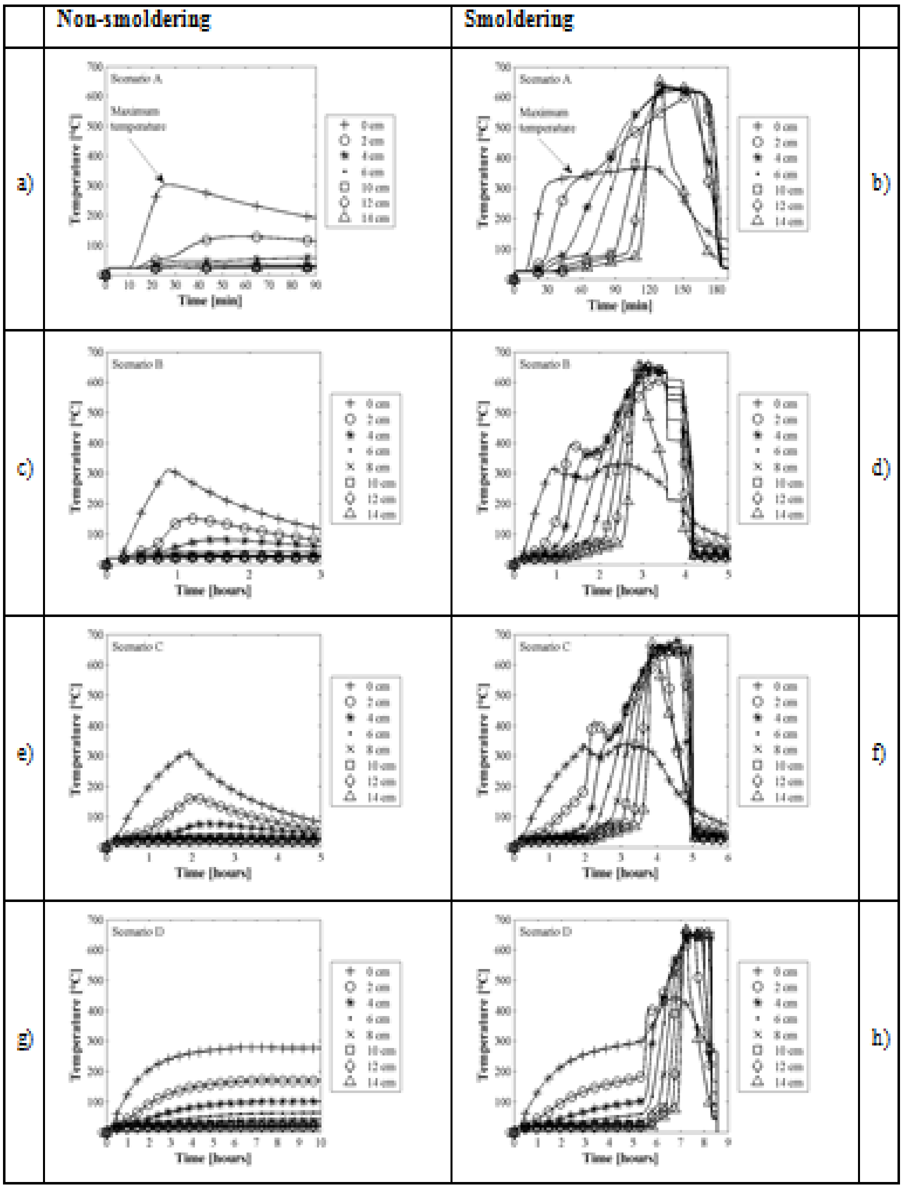


**Figure 3:** Temperature as a function of time and position for scenario A-D for both non-smoldering (left column) and smoldering cases (right column). The temperature was measured at the hotplate (0 cm) as well as at a series of different heights above it, as indicated. The density was 100 kg/m³. Some data is missing after maximum has been reached for scenario B in part d) Hagen and his colleagues [7].

**Table 1:** Time and temperature for onset of smoldering in cotton with density 100 kg/m³ Hagen and his colleagues [7]

| Scenario | Ignition Temperature (°C) | Ignition time (min) |
|---|---|---|
| A | 303 ± 2 | 18 |
| B | 313 ± 2 | 41 |
| C | 314 ± 2 | 99 |
| D | 284 ± 5 | 256 |

## 3. Simulation input and ignition models

### *3.1 Comsol*

To calculate the temperature in the cotton sample a multi physics model called Comsol is used. In this article only the grid generator and heat-transfer-model will be used.

The grid used during the simulations is a free tetrahedral mesh. Details regarding the grid generation and solving the equations for the system in Comsol are found in the reference manual of the program. In the simulations only heat transfer is accounted for since the focus of this article is onset of smoldering. If the smoldering process after onset of smoldering is to be investigated, more elaborate models must be incorporated, including chemical kinetics. The heat transfer within the system is based on the general heat transfer equation [11]:

$$\rho c_p \frac{\partial T}{\partial t} - \nabla(\lambda \nabla T) - \dot{Q} = 0 \tag{6}$$

where the first part of the equation describes the stored energy, the second part describes the energy transport in and out of the system and the last part is a source term describing energy production within the system.

At the surface of the system the heat loss is calculated using both convection and thermal radiation:

$$\dot{q}''_{conv} = h(T_s - T_a) \tag{7}$$

$$\dot{q}''_{rad} = \varepsilon\sigma(T_s^4 - T_a^4) \tag{8}$$

where $\dot{q}''$ is the energy loss pr. area and time, $h$ is the convective heat transfer coefficient, $T_s$ is the surface temperature and $T_a$ is the ambient temperature, $\varepsilon$ is emissivity and $\sigma$ is Stefan-Boltman constant.

Appendix A.1 shows the results of a grid sensitivity-analysis performed to determine the appropriate grid size. A grid with maximum grid size of 0.004 m and minimum grid size of $2\cdot10^{-5}$ m has been used for the simulations.

### *3.2 Material data*

The modeling of onset of smoldering will be done using material properties found in the literature, and the results will be compared with the experimental results described in sec. 2.2.2.

Material properties are given in tables 2 to 4. Materials properties for the hotplate, insulation and gypsum are assumed to be constant with temperature, while the properties for cotton will change with density and temperature.

#### *3.2.1 Hotplate, insulation and gypsum*

**Ceramic tiles**

The hotplate consists of three ceramic tiles. The material values for the tiles are found in literature [12] and adjusted to give the same temperature development on top of the hotplate as recorded for the experiments described in sec. 2.2.2. The values are given in table 2.

**Table 2:** Properties for the hotplate

| | Ceramic tiles | Insulation | Gypsum |
|---|---|---|---|
| Density (ρ) | 2430 kg $m^{-3}$ | 128 kg $m^{-3}$ | 1440 kg $m^{-3}$ |
| Conductivity (k) | 1.0 $Wm^{-1}K^{-1}$ | 0.15 $Wm^{-1}K^{-1}$ | 0.48 $Wm^{-1}K^{-1}$ |
| Specific heat ($C_p$) | 1150 J $kg^{-1}K^{-1}$ | 1090 J $kg^{-1}K^{-1}$ | 840 J $kg^{-1}K^{-1}$ |
| Reference | Adapted from [12] and from our own measurements | [13] | [13] |

**Insulation:**

The insulation, which is Kawool blanket (Standard 1260 °C), is used to insulate the sides and bottom of the hotplate. The insulation is 0.025 m thick on the sides and 0.02 m thick at the bottom of the hotplate. The material values are given in table 2.

**Gypsum:**

A gypsum plate (0.3 m·0.3 m·0.01 m) forms a protection layer between the experiment and a scale used for weighing the sample. The material values are given in table 2.

#### *3.2.2 Cotton*

Information on temperature-dependent material properties for cotton with absorbed water is scarce.

Approximate values are obtained by combining values for dry cotton and water. Material values for dry cotton is given in table 3.

The temperature-dependent conductivity of cotton is calculated using:

$$k = (1-\gamma)\cdot k_{\text{cotton}} + \gamma \cdot k_{\text{moisture}} \tag{9}$$

where $\gamma$ is the fraction of moisture, $k_{\text{cotton}}$ is conductivity of dry cotton and $k_{\text{moisture}}$ is conductivity of water. The values for conductivity are given in table 4. The conductivity of dry cotton ($k_{\text{cotton}}$) is assumed to be constant as function of temperature, but dependent on density [14]. In table 4 properties for water at three different temperature regions are given. It is assumed that moisture evaporates at a constant rate between 50 and 80 °C and that its effects on conductivity and specific heat are reduced systematically with increasing temperature.

**Table 3:** Material properties for cotton

| Property | Reference |
|---|---|
| $h = 10$ W m$^{-2}$ K$^{-1}$ | [11] |
| $k_{\rho=100} = 0.044$ Wm$^{-1}$K$^{-1}$ | Extrapolated from Tye [14] |
| $\varepsilon = 0.9$ | |
| $R = 8.31431$ J K$^{-1}$ mol$^{-1}$ | |
| $T_a = 288 - 295$ K | Case dependent |
| $\rho = 100$ kg m$^{-3}$ | Density of cotton |

**Table 4:** Assumed material properties for cotton and water as a function of temperature

| Dry cotton | | |
|---|---|---|
| Conductivity | $k_{\text{cotton}} = 0.044$ W/(m·K) | |
| Specific heat | $c_{p,\text{cotton}} = (1075+4.27\cdot(T[K]-293))$ J/(kg·K) | |
| Water | | |
| Temperature region | Conductivity W/(m·K) | Specific heat J/(kg·K) |
| T< 323 K | $k_{\text{moisture}} = 0.62$ | $c_{p,\text{moisture}} = 4181$ |
| 323K ≤ T < 353 K | $k_{\text{moisture}} = 0.62-0.02067\cdot(T[K]-323)$ | $c_{p,\text{moisture}} = 81122$ |
| 353 K ≤ T | $k_{\text{moisture}} = 0$ | $c_{p,\text{moisture}} = 0$ |

The specific heat of dry cotton increases linearly with temperature as reported by Hatakeyama and his colleagues [15]. These results were reported to be valid only from 50 °C, due to effects of moisture. In this article the results of Hatakeyama and his colleageswill be used from 20 °C, since the effect of water absorbed in the cotton will be treated separately. The temperature-dependent specific heat of dry cotton is [15]:

$$c_{p,\text{cotton}} = (1075 + 4.27\cdot(\mathrm{T}[\mathrm{K}] - 293))\frac{\mathrm{J}}{\mathrm{kg}\cdot\mathrm{K}} \tag{10}$$

The apparent specific heat for absorbed water results from both heating and vaporization. An approximation for the specific heat of the moisture within the cotton is made (see table 4):

$$c_{p,\text{moisture}} = \frac{\text{Enthalpy}}{\text{Temperature}} = \frac{\Delta h}{\Delta T} \tag{11}$$

- Water heated from room temperature (20°C) to 50 °C [16]:

$$c_{p,\,moisture:\,20\text{-}50°\text{C}} = \frac{209.34 - 83.915}{30} \cdot 10^3 \frac{\text{J}}{\text{kg} \cdot \text{K}} = 4181 \frac{\text{J}}{\text{kg} \cdot \text{K}} \tag{12}$$

- Water heated and evaporated between 50 °C to 80 °C [16]:

$$c_{p,\text{moisture: 50-80°C}} = \frac{2643.0 - 209.34}{30} \cdot 10^3 \frac{\text{J}}{\text{kg} \cdot \text{K}} = 81122 \frac{\text{J}}{\text{kg} \cdot \text{K}} \tag{13}$$

The resulting values for overall specific heat and conductivity for cotton with absorbed water are illustrated in figure 4. The model used is a pure heat-transfer-model, water vapor transport has therefore not been included. By not including water vapor an error of maximum 5% is introduced to $k_{cotton}$ and $C_{p,\,cotton.}$ The density of cotton is also affected by the evaporation of water [17]. In this article, it is assumed that the weight is reduced accordingly to the loss of water as the temperature exceeds 80 °C [9].

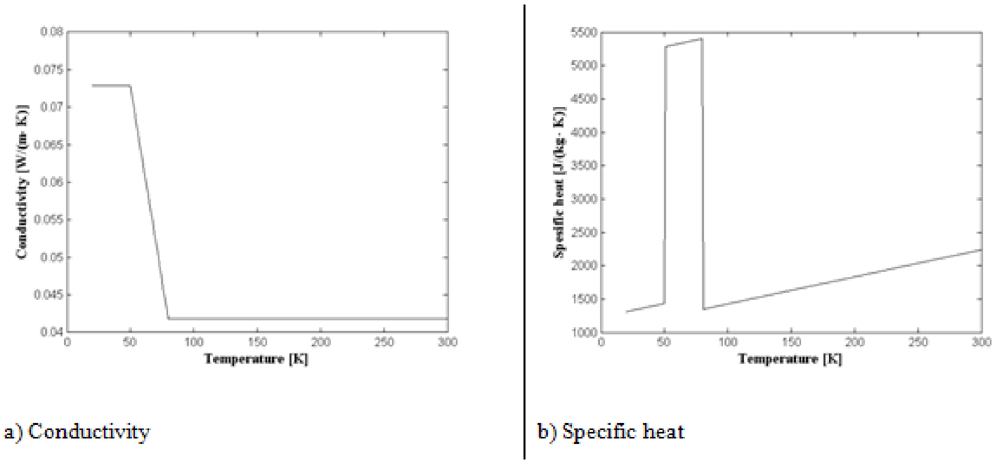


**Figure 4:** Conductivity and specific heat as a function of temperature for cotton with density of 100 kg/m³ containing 5% water by weight.

Cotton is also different from the other materials used in the experiments described by Hagen and his colleagues [7], since it produces energy as it decomposes at higher temperatures. From the work done by Jones [18], Cabrales and Abidi [19], Shafizadeh and Bradbury [20], heat production based on an Arrhenius equation can be developed. However, material values to be used during simulations are not easily found, since both the pre-exponential-factor (A*) and the activation energy ($E_a$) are difficult to establish from experimental results.

In this paper the heat production rate used in the 3D-simulations is based on work done by Wanke and Krause at Otto-von-Guericke Universität in Magdeburg, Germany [21]. They determined the heat release rate for cotton as a function of temperature using a DSC-analysis (Differential Scanning Calorimetry). In COMSOL heat release rate pr. unit volume is used, and the results from Wanke and Krause have been modified according to this (See figure 5).

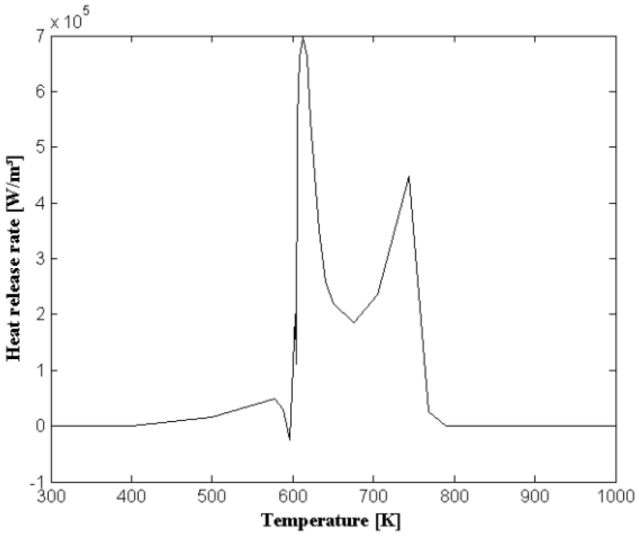


**Figure 5:** Heat release rate pr. unit volume as a function of temperature for cotton with density 100 kg/m³. The heat release rate is modified from results from Wanke and Krause [21].

### *3.3 Ignition models*

In this article two approaches to estimate onset of smoldering fire will be investigated. The first is a 1D-ignition model based on the work done by Bowes and Townsend as described in section 2.1 [8]. The second is a 3D-ignition model that uses a runaway reaction as the indicator of onset of smoldering.

#### *3.3.1 1D-ignition model*

The one dimensional (1D) ignition model is based on the description in section 2.1. The ignition temperature ($T_p$) is found using eq. 5. For every time-step the height (*l*) is determined using the simulated centerline temperature from the 3D-simulations in COMSOL. When *l* is found (that is where the cotton temperature is equal to 40 °C), the height of the reaction zone ($l_R$) can be calculated using adaptations of eq. 3 (see next paragraph), and the heat production can be worked out using eq. 2.

The heat production in this 1D-ignition model is estimated using an Arrhenius approximation, where the activation energy (Ea) is 102 $J \cdot mol^{-1}$ [18] and heat of combustion $17.3 \cdot 10^6$ $J \cdot kg^{-1}$ [22].

The pre-exponential factor (A*) is estimated to $5.0 \cdot 10^{11}$ $s^{-1}$ using the data from Wanke and Krause (see figure

5). For temperatures under 250 °C, the heat production is assumed to be so small that it can be ignored.Eq. 3 assumes a linear temperature gradient in the heated material. However, as discussed by Thomas and Bowes [10], the temperature with in the sample have different profiles depending on the heat flux scenario. For a rapid heating of the sample, see scenario A in figure 3a and b, the heat from the hotplate will be the most significant contributor of energy and the temperature profile will have a decreasing trend as the height above the hotplate increases. The temperature profile for scenario A with a hotplate temperature of 303 °C is shown in figure 6a. For a slow heating of the sample, see scenario D in figure 3g and h, the energy production in the sample will be more pronounced when approaching onset of smoldering. The increase in energy production in the sample will result in higher temperatures in the sample itself compared with the hotplate temperature. The temperature profile for scenario D at a hotplate temperature of 293 °C is shown in figure 6b. In order to account for the two temperature profiles introduced by Thomas and Bowes [10], three different variations of the 1D-model are used to evaluate the temperature for onset of smoldering. The first model (1D-a) uses only the hotplate temperature to determine the onset of smoldering, while the second model (1D-b) uses the maximum temperature in the cotton. See table 5a and 5b for details on the temperature profile and reaction zone. The third model (1D-c) uses the same temperature as the hotplate temperature to determine the temperature gradient of the system. However, it is important to notice that this temperature ($T_{p*}$) is found above the position of the maximum temperature.There is also an addition to the reaction zone as energy is produced in the volume with temperatures from $T_{max}$ to $T_{p*}$. The model is illustrated in the figure in 5c. The energy produced in the volume limited by temperatures from $T_p$ to $T_{max}$ is assumed to move towards the hotplate and therefore not affecting the onset of smoldering. This in accordance with the work of Thomas and Bowes [10].

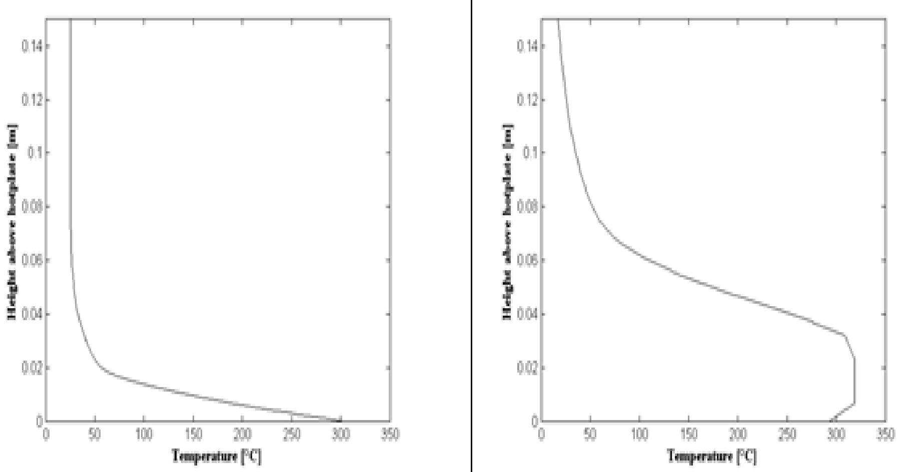


a) Rapid heating of sample: Scenario A with a hotplate temperature of 300 °C.

b) Slow heating of sample: Scenario D with a hotplate temperature off 293 °C

**Figure 6:** Temperature profile in sample according to heating scenario for cotton with density 100 kg/m³.

**Table 5:** Models for reaction zone calculations

| 1D-modell | Temperature profile | Temperature gradient | Reaction zone |
|---|---|---|---|
| a | 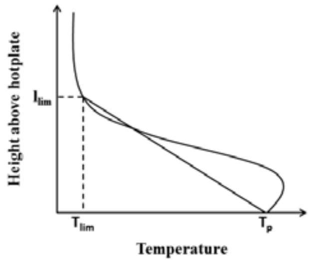 | $b = \frac{T_P - T_{\lim}}{l_{\lim}}$ | $l_R = \frac{RT_P^{\ 2}}{bE}$ |
| b | 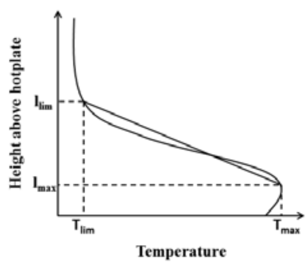 | $b = \frac{T_{\max} - T_{\lim}}{l_{\lim} - l_{\max}}$ | $l_R = \frac{RT_{\max}^{\ 2}}{bE}$ |
| c | 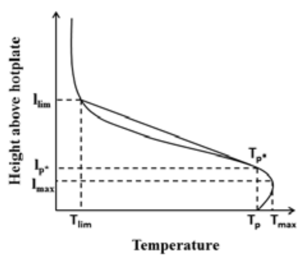 | $b = \frac{T_{P^*} - T_{\lim}}{l_{\lim} - l_{p*}}$ | $l_R = \frac{RT_{P^*}^{\ 2}}{bE} + \left(l_{p*} - l_{\max}\right)$ |

### *3.3.2 3D-ignition model*

The 3D-ignition model will use the COMSOL simulation results directly. To find the temperature for onset of fire the simulations will follow same approach as described by Hagen and his colleagues [7]. In Hagen and his colleagues– method the hotplate is heated to a pre-determined temperature (the cut-off temperature) and then the power to the hotplate is switched off. For a non-smoldering case the hotplate will increase in temperature, reaching a maximum temperature and then cool off (see figure 3).

A series of cut-off temperatures vs. max temperatures are plotted against each other (see figure 7), and from the results a linear fit for the non-smoldering cases is found. The linear fit is used to find a lower and upper bound for an ignition temperature interval.

Using the linear fit and the cut-off temperature for the last non-smoldering case, $T_{low}$ is estimated as a lower bound for the ignition interval. Similarly, the upper bound for the ignition interval ($T_{high}$) can be found using the linear fit and the cut-off temperature giving onset of smoldering. In figure 10 the method is illustrated using results for the simulation of scenario A. Using the linear fit for simulated results, a temperature interval for onset of smoldering for scenario A can be estimated between 315 and 322 °C or 319 °C ± 3 °C.

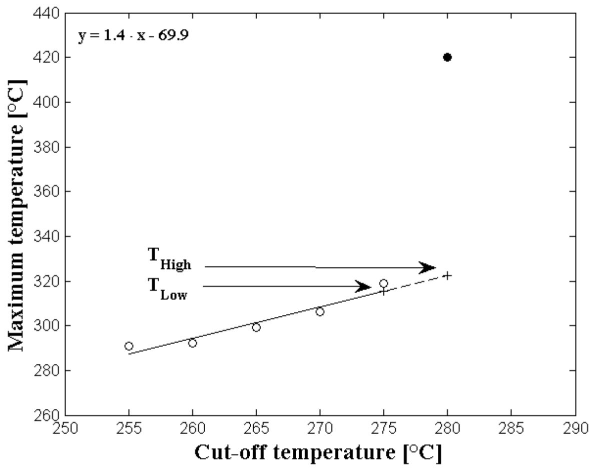


**Figure 7:** Simulated maximum hotplate temperature as a function of cut-off temperature for heating scenario A. The cotton had a density equal to 100 kg/m³. The smoldering case is indicated by a solid circle (•), while the non-smoldering cases are indicated by a circles (○). $T_{High}$ and $T_{Low}$ are indicated by crosses (+).

## 4. Results

### *4.1 Simulation vs. experimental results*

The results from the simulations are shown in table 6. The results from the simulation show an overall good correlation with the experimental results until onset of smoldering. After the onset of smoldering the simulations overestimate the temperatures in the cotton, which is expected since the model does not account for the oxygen transport or the chemical reaction in the cotton. In order to simulate smoldering the model must be developed further to include chemical kinetics, permeability and inflow of oxygen. There are also some minor differences due to differences in the moisture contents of the cotton and small changes in the power output from the hotplate as the heat resistance in the hotplate changes with temperature. The effects of moisture in the simulations are discussed in Appendix A.2 .

### *4.2 Time and temperature for onset of smoldering*

As described in chapter 3, four models for onset of smoldering will be tested: three linear models and a finite element model.

The linear models are based on the temperature gradient calculated by the COMSOL model, while the finite element model is based on a calculated run-away reaction in the COMSOL model. The estimated time and temperature for onset of smoldering are shown in table 7.

The three linear ignition models (1D-a-b-c) estimate the temperature for onset of smoldering to within 0 – 6 % of the experimental results, while the time to onset is estimated to within 3 – 60 %. The 3D-ignition model estimates the temperature for onset of smoldering to within 2-5 % of the experimental results, while the time to onset is estimated within 0 – 26 %.

**Table 6:** Results of experiments and simulations

<table>
<tr><th>Scenario</th><th>Experimental results</th><th>Simulated results</th></tr>
<tr><td>A</td><td>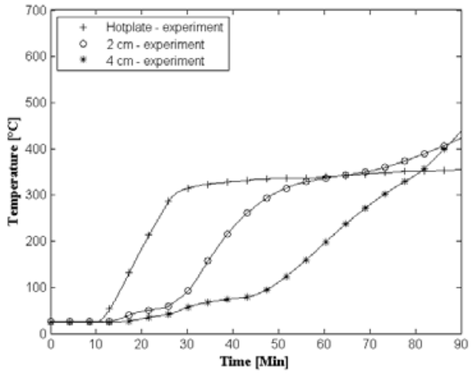
</td><td>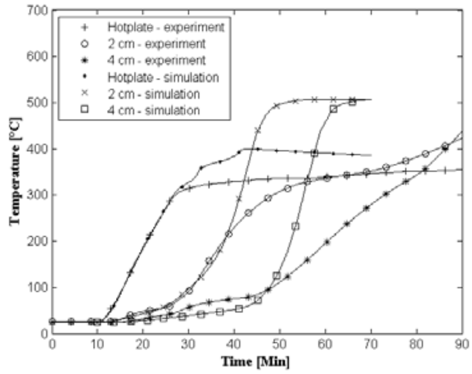
</td></tr>
<tr><td>B</td><td>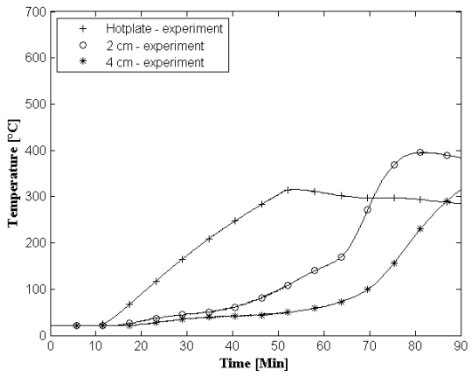
</td><td>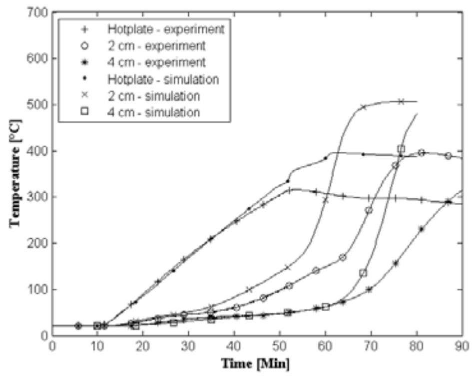
</td></tr>
<tr><td>C</td><td>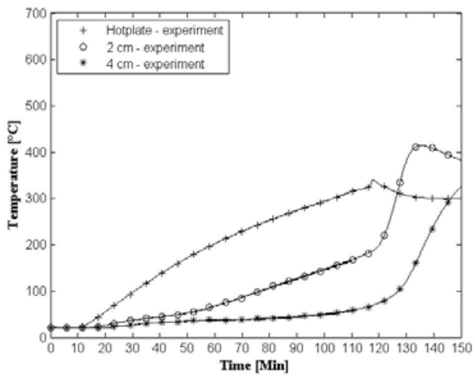
</td><td>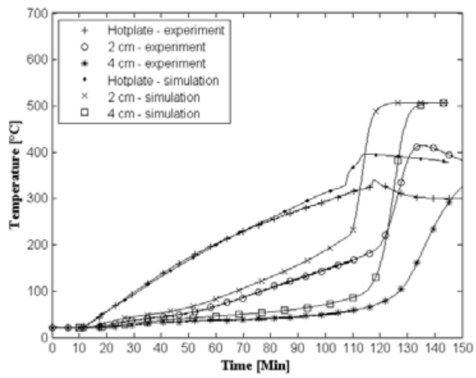
</td></tr>
<tr><td>D</td><td>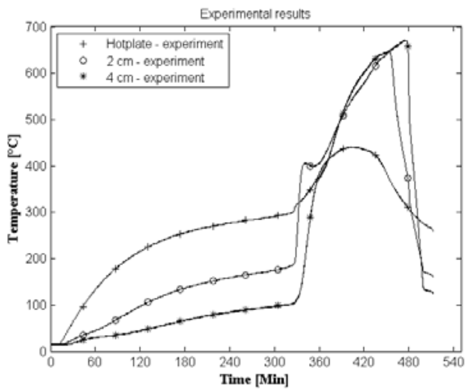
</td><td>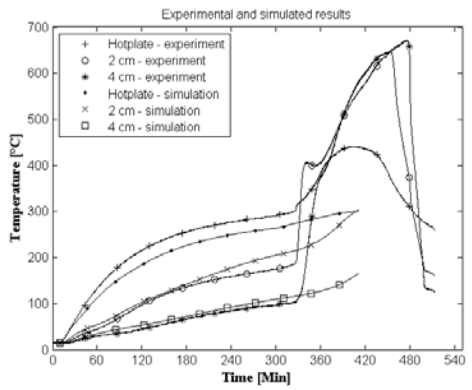
</td></tr>
</table>

**Table 7:** Estimated time and temperature for onset of smoldering in cotton samples when subjected to different heating scenarios. The cotton had a density of 100 kg/m³

| | Experimental results | | Simulated results | | | | | | | | | |
|---|---|---|---|---|---|---|---|---|---|---|---|---|
| | | | Linear model 1D-a† | | Linear model 1D-b† | | Linear model 1D-c† | | Finite model | | | |
| Scenario | Temperature (°C) | Time (min) | Temperature (°C) | Time (min) | Temperature (°C) | Time (min) | Temperature (°C) | Time (min) | Temperature (°C) | Time (min) | Error Temp. (%) | Error Time (%) |
| A | 303 ± 2 | 18 | 305 | 27 | 305 | 27 | 304 | 26 | 319 ± 3 | 18 | 5 | 0 |
| B | 313 ± 2 | 41 | 313 | 48 | 313 | 48 | 311 | 47 | 321 ± 3 | 39 | 3 | 5 |
| C | 314 ± 2 | 99 | 305 | 96 | 305 | 96 | 303 | 95 | 324 ± 2 | 97 | 3 | 3 |
| D | 284 ± 5 | 256 | 300 | 402 | 302 | 371 | 296 | 407 | 278 ± 8 | 323 | 2 | 26 |
| | | | | | | | | | | | | |

† $T_{lim}$ is 40 °C, see appendix A.3 for sensitivity of $T_{lim}$.

## 5. Discussion

The simulated results presented in section 4, figure 6, show a good correlation between the experimental and simulated results. Since the simulations in COMSOL only account for heat-transfer, the results can only be used to estimate the onset of smoldering. If smoldering processes are to be simulated, more complex models must be developed as described among others by Chen, Rein and Liu [6].

In general both the 1D-ignition-models and the 3D-ignition-model predict the temperature for onset of smoldering to within 2-6 % of the experimental results, or within 6-16 °C of the experimental result. The 3D-ignition-model over-predicts the temperature to onset of smoldering. However, it has the same trends as the experimental results with higher temperatures for scenario A, B and C and lower temperature for scenario D. The 1D-ignition-models do not follow the same trend and the results are less systematic compared with the 3D-ignition-model.

Compared to the uncertainties of the experimental results, the simulated results of the temperature for onset of smoldering are rather good. The estimated time to onset of smoldering for scenario A, B and C is within 5 % (or 2 minutes) of the experimental result using the 3D-ignition-model and 3-50 % (3-9 minutes) using the 1D-ignition-models. The time estimates for scenario D are poorer and varies between 26 % (or 69 minutes) using the 3D-ignition-model and 45-59 % (115-151 minutes) using the 1D-ignition-models. From results of scenario D, it seems as if permeability, convection heat transfer and heat production within the cotton are not properly accounted for in the simulations due to the large deviation between experimental and simulated results.

It was expected that model 1D-c would have better time and temperature estimates for onset of smoldering for scenario D since the temperature profile of Thomas and Bowes [10] is included in the model. The results in table 7 show that model 1D-c is only marginally better than models 1D-a og –b. The reaction layer ($l_R$) is very thin, and the small differences in the calculated $l_R$-values for the different models give only marginal differences in the temperature. In practical application a simpler 1D-model (1D-a) seems to be sufficient to estimate the onset of smoldering using models based on Bowes and Townsend’s work [8].

The material values are taken from available literature and combined to be used in the different simulations. It is interesting to see the good correlation between experimental and simulated results even when the material values are combined in this way. The heat production of the cotton must be investigated closer, but it is clear from the data from Wanke and Krause [21] that cotton is a very complex material and its heat production is strongly temperature-dependent.

As a concluding remark it is interesting to observe how the 3D-heat-transfer-model is able to follow the trends of the experimental results with respect to temperature and time to onset of smoldering. The 3D-model will be able to simulate situations where onset of smoldering cannot be evaluated using 1D-appoximations. This together with models which can include permeability and chemical kinetics make the 3D-models interesting for use in more practical engineering applications.

## 6. Conclusion

In this article a finite element heat-transfer model (Comsol) was used to estimate the temperature profile within a cotton sample. From the estimated temperature profiles, the time and temperature for onset of smoldering were investigated using one dimensional (1D) and three dimensional (3D) models. A comparison of the simulated results with the experimental results shows that the temperature for onset of smoldering can be estimated to within 2-5 % of the experimental results, or within 6-16 °C, using a 3D-ignition model. The time to onset can be estimated to within 5 % (or 2 minutes) of the experimental result for high heat flux scenarios. For the low heat flux scenario the time estimate is poorer and within approximate 26 % of the experimental results. The results from the 1D-models are poorer and less systematic compared with the 3D-model.The results presented here show that simulations of onset of smoldering can be performed using pure 3D-heat-transfer-models. The model used here are easy to implement and to use in more practical engineering applications.

**Acknowledgements**

The work described in this paper was in part funded by The Research Council of Norway (NFR), project 238329: Emerging Risks from Smoldering Fires (EMRIS - collaboration).

## 7. Nomenclature

$A^*$ pre-exponential factor ($s^{-1}$)

$b$ negative slope of the linear temperature profile (K $m^{-1}$)

$cp$ Specific heat (J $kg^{-1}$ $K^{-1}$)

| | |
|---|---|
| $E_a$ | activation energy (J $mol^{-1}$) |
| $\Delta H_C$ | heat of combustion (J $kg^{-1}$) |
| $h$ | convective heat transfer coefficient (W $m^{-2}$ $K^{-1}$) |
| $k$ | thermal conductivity ($Wm^{-1}K^{-1}$) |
| $l$ | characteristic length (m) |
| $l_R$ | reaction layer thickness (m) |
| $R$ | universal gas constant (J $K^{-1}$ $mol^{-1}$) |
| $T_a$ | ambient temperature (K) |
| $T_p$ | hotplate temperature (K) |
| $\Delta\tau$ | Time step (s) |
| $\dot{q}''$ | heat flux pr. area (W $m^{-2}$ ) |
| $\dot{q}'''$ | heat production pr. volume (W $m^{-3}$ ) |
| $\dot{Q}$ | heat production (W) |
| $\gamma$ | fraction of moisture (-) |
| $\varepsilon$ | emissivity (-) |
| $\rho$ | density ($kg/m^3$) |
| $\sigma$ | Stefan-Boltman constant (W $m^{-2}$ $K^{-4}$) |

## 8. Appendix A: Sensitivity

### *A.1 Grid sensitivity*

The 3D-heat-transfer-model used is based on a finite element method, as described in section 2. The mesh used is tetrahedral, where the grid size and the number of elements used are described in table A.1. The simulation program comes with pre-defined grid sizes, which are used here. In addition two customary meshes are introduced. The model has been run with different grid sizes in order to look at the effects of grid sizes on ignition time and temperature. In all 11 different grid sizes have been investigated. When testing the grid size, scenario A has been used with a moisture content of 5 % and density 100 kg/m³. The results in table A.1 show that a grid size less than extremely fine gives stable results. Custom #1 mesh is used for all presented simulations in the article.

**Table 8:** Element and grid size

| Description | Maximum element size | Minimum element size | Numbers of elements | Minimum element quality |
|---|---|---|---|---|
| | (m) | (m) | | |
| Custom #2 | 0.0030 | 1.0 E-5 | 3213133 | 0.1253 |
| Custom #1 | 0.0040 | 2.0 E-5 | 1352903 | 0.1132 |
| Extremely fine | 0.0060 | 6.0E-5 | 372662 | 0.1577 |
| Extra fine | 0.0105 | 4.5E-4 | 73941 | 0.09724 |
| Finer | 0.0165 | 0.0012 | 26632 | 0.1338 |
| Fine | 0.024 | 0.0030 | 14509 | 0.1028 |
| Normal | 0.03 | 0.0054 | 10082 | 0.09526 |
| Coarse | 0.045 | 0.0084 | 5910 | 0.02472 |
| Coarser | 0.057 | 0.012 | 3801 | 0.02674 |
| Extra coarse | 0.09 | 0.0162 | 1953 | 0.006037 |
| Extremely coarse | 0.15 | 0.021 | 852 | 0.0002267 |

**Table 9:** Ignition time and temperature as function of mesh size for cotton with density 100 kg/m³ and a moisture contents of 5%.

| | Scenario A | |
|---|---|---|
| Mesh size | Ignition temperature | Ignition Time |
| | (°C) | (s) |
| Custom #2 | 318 ± 3 | 1077 |
| Custom #1 | 319 ± 3 | 1076 |
| Extremely fine | 311 ± 3 | 1062 |
| Extra fine | 321 ± 3 | 1093 |
| Finer | 338 ± 6 | 1196 |
| Fine | 322 ± 4 | 1125 |
| Normal | 328 ± 4 | 1127 |
| Coarse | 322 ± 4 | 1148 |
| Coarser | * | * |
| Extra coarse | * | * |
| Extremely coarse | * | * |
| * The ignition temperature exceeded 350 °C and the simulation was terminated. | | |

***A.2 Moisture contents***

In the work done by Hagen and his colleagues [7], the moisture contents were estimated to 5% based on previous experiments. The amount of moisture in the cotton is affected by temperature and humidity in the surrounding air. Here the effects of different amounts of moisture will be investigated by varying the fraction of moisture $\gamma$ in the cotton as described in eq. 9. The contents of moisture in the cotton will be varied from 0 to

10%. The Custom #1 mesh will be used with scenario A and density 100 kg/m³. The effect of moisture on the simulated time and temperature of onset of smoldering is small and in the range from 2 to 9 % of the experimental results. The overall effects of moisture in the simulations of time and temperature for onset of smoldering are small.

**Table 10:** Ignition time and temperature as function of moisture contents in the cotton. The cotton density is 100 kg/m³ and Custom # 1 mesh is used.

| | Scenario A | |
|---|---|---|
| Amount of moisture | Ignition temperature | Ignition time |
| (%) | (°C) | (s) |
| 0 | 311 ± 2 | 1050 |
| 1 | 315 ± 3 | 1071 |
| 2 | 316 ± 3 | 1070 |
| 3 | 318 ± 4 | 1078 |
| 4 | 319 ± 4 | 1080 |
| 5 | 319 ± 3 | 1076 |
| 6 | 331 ± 4 | 1125 |
| 7 | 311 ± 4 | 1077 |
| 8 | 313 ± 4 | 1083 |
| 9 | 314 ± 4 | 1084 |
| 10 | 315 ± 4 | 1086 |
| | | |

### *A.3 Limiting temperature*

Using the 1D-ignition models described in section 3.3.1, a sensitivity analysis on the variable $T_{lim}$ has been performed. $T_{lim}$ has been investigated for values $T_{ambient}$ (room temperature at the time of experiment), 30, 35, 40 and 45 °C. In table A.4 the estimated temperatures for onset of smoldering are shown. $T_{lim}$ of 35, 40 and 45 °C gave the same overall accuracy and $T_{lim}$ of 40 °C was decided to use for comparison with earlier work [7].

**Table 11:** Sensitivity analysis of $T_{lim}$ for 1D-ignition models. The cotton density is 100 kg/m³ and Custom # 1 mesh is used.

| | | $T_{lim}$ | | | | | | | | | | | | | | |
|---|---|---|---|---|---|---|---|---|---|---|---|---|---|---|---|---|
| | | $T_{ambient}$ | | | 30 | | | 35 | | | 40 | | | 45 | | |
| Scenario | Experimental results | 1D-a | 1D-b | 1D-c | 1D-a | 1D-b | 1D-c | 1D-a | 1D-b | 1D-c | 1D-a | 1D-b | 1D-c | 1D-a | 1D-b | 1D-c |
| A | 303 ± 2 | 305 | 305 | 304 | 312 | 312 | 310 | 315 | 315 | 313 | 317 | 317 | 313 | 319 | 319 | 313 |
| B | 313 ± 2 | 299 | 299 | 298 | 307 | 307 | 305 | 309 | 309 | 308 | 311 | 311 | 309 | 313 | 313 | 311 |
| C | 314 ± 2 | 294 | 294 | 293 | 301 | 301 | 300 | 303 | 303 | 302 | 305 | 305 | 304 | 307 | 307 | 305 |
| D | 284 ± 5 | 293 | 293 | 290 | 298 | 299 | 294 | 299 | 301 | 295 | 300 | 301 | 296 | 301 | 303 | † |
| | | | | | | | | | | | | | | | | |
| | | | | | | | | | | | | | | | | |
| † No estimate of onset was achieved here. | | | | | | | | | | | | | | | | |

## References


[1] V Babrauskas, Ignition Handbook: Principles and Applications to Fire Safety Engineering, Fire Investigation, Risk Management and Forensic Science, Fire Science Publishers/SFPE, Issaquah, WA, 2003.

[2] G Rein, Smoldering Combustion, in: Hurley MJ (Ed.), SFPE handbook of fire protection engineering, 5th ed., Springer, New York, 2016, pp. 581-603.

[3] TJ Ohlemiller. Cellulosic Insulation Material. III. Effects of Heat-Flow Geometry on Smolder Initiation, Combustion Science and Technology. 26 (1981) 89-105.

[4] Suhendra, Schmidt, Krause, Underground Coal Fire Extinction Model using Coupled Reactive Heat and Mass Transfer Model in Porous Media, (2009).

[5] AB Dodd, C Lautenberger, C Fernandez-Pello. Computational modeling of smolder combustion and spontaneous transition to flaming, Combustion and Flame. 159 (2012) 448-461.

[6] H Chen, G Rein, N Liu. Numerical investigation of downward smoldering combustion in an organic soil column, International Journal of Heat and Mass Transfer. 84 (2015) 253-261.

[7] BC Hagen, V Frette, G Kleppe, BJ Arntzen. Effects of heat flux scenarios on smoldering in cotton, Fire Safety Journal. 61 (2013) 144-159.

[8] PC Bowes, SE Townshend. Ignition of Combustible Dusts on Hot Surfaces, British Journal of Applied Physics. 13 (1962) 105-114.

[9] BC Hagen, V Frette, G Kleppe, BJ Arntzen. Onset of smoldering in cotton: Effects of density, Fire Safety Journal. 46 (2011) 73-80.

[10] Thomas, Bowes, Thermal Ignition in a Slab With One Face at a Constant High Temperature, Trans.Farad.Soc. 57 (1961) 2007.

[11] JP Holman, Heat transfer, 7th ed., McGraw-Hill, London, 1992.

[12] Effting, Alarcon, Güths, Novaes de Oliveira, Paschoal, Influence of porosity on thermal properties of ceramic floor tiles, (2006) 409.

[13] SIG Technical Insulation, Kaowool Blanket.pdf - SIG Technical Insulation, 2014.

[14] RP Tye. Heat Transmission in Cellulosic Fiber Insulation Materials, Journal of Testing and Evaluation. 2 (1974) 176.

[15] T Hatakeyama, K Nakamura, H Hatakeyama. Studies on Heat-Capacity of Cellulose and Lignin by Differential Scanning Calorimetry, Polymer. 23 (1982) 1801-1804.

[16] Y Çengel A., Thermodynamics: an engineering approach, 6th ed., McGraw-Hill, Boston, 2007.

[17] E Corradini, EM Teixeira, PD Paladin, JA Agnelli, ORRF Silva, LHC Mattoso. Thermal stability and degradation kinetic study of white and colored cotton fibers by thermogravimetric analysis RID C-4755-2012, Journal of Thermal Analysis and Calorimetry. 97 (2009) 415-419.

[18] JC Jones, GC Wake. Measured Activation-Energies of Ignition of Solid Materials, Journal of Chemical Technology and Biotechnology. 48 (1990) 209-216.

[19] L Cabrales, N Abidi. On the thermal degradation of cellulose in cotton fibers, Journal of Thermal Analysis and Calorimetry. 102 (2010) 485-491.

[20] F Shafizadeh, AGW Bradbury. Smoldering Combustion of Cellulosic Materials, Journal of Building Physics. 2 (1979) 141-152.

[21] Wanke, Krause, Energy production of cotton as a function of temperature, (2015).

[22] JC Jones. Thermal Calculations on the Ignition of a Cotton Bale by Accidental Contact with a Hot Particle, Journal of Chemical Technology and Biotechnology. 65 (1996) 176-178.